NURETH14-90

SUDDEN DISCHARGE OF GAS MIXTURE IN A CONFINED MULTI-COMPARTMENT

D. Paladino, G. Mignot, N. Erkan, R. Zboray, R. Kapulla, M. Andreani

Laboratory for Thermal Hydraulics, Nuclear Energy and Safety Research Department CH-5232 Villigen PSI Paul Scherrer Institut

Abstract

The paper presents the results of a series of tests in the PANDA facility, performed within the OECD/SETH-2 project, focusing on the evolution of gas distribution in one subdivided compartment resulting from the sudden opening of a connection with a second compartment initially at higher pressure and filled with a mixture of different composition. This situation occurs in the case of the sudden opening of a rupture disk (or hatches) – and could be related to the EPR design. Gas transport mixing and distribution within the containment compartments is driven by the pressure difference between the volumes in the early phase of the test, and by temperature gradient and gas mixture concentration difference after that the pressure between the vessels has been equalized. The analysis performed with GOTHIC code and presented in this paper aims at complementing the interpretation of the physical phenomena taking place during the test evolution and inferred from the measurement results.

1. Introduction

The OECD/SETH-2 project investigations are devoted to LWR containment safety. The project has been carried out in the 2007-2010 period at PSI (PANDA Facility in Switzerland) and CEA (MISTRA Facility in France) with the aim of generating high-quality experimental data suitable for improving the modeling and for Lumped Parameter and 3D (CFD) codes validation [1].

The PANDA program consists of six test series focusing on hydrogen (in PANDA helium is used to simulate hydrogen) stratification break-up induced by mass sources, e.g. vertical fluid release (jet or plume, series identified in the SETH-2 project as ST1) [2], [3] and horizontal fluid release (ST2) [4], [5] heat sources (simulating the energy generated by hydrogen-oxygen recombiner operation) (ST5) or heat sinks (due to condensation of steam caused by containment coolers (ST4) [6], [7] or sprays (ST3), [8], [9].

The paper presents the PANDA experimental results and the analysis of a series of PANDA tests which focuses on the evolution of gas distribution in two large volumes, having initially different gas composition and different pressures and after being suddenly connected (ST6). This situation occurs in the case of the sudden opening of a rupture disk and could be directly related to the EPR design [10]. In this design, the presence of "rupture foils" that could burst under pressure difference might lead to mixing process similar to the one expected in this test series. The pressure differential used in the ST6 series, however, is not prototypical or representative of the current EPR design. In addition, data related to the mixing of fluids with initially different densities in two adjacent volumes as the result of the sudden opening of an aperture are rather scanty, and do not encompass data at large scale.

Gas transport mixing and distribution within the containment compartments is driven by the pressure difference between the two large volumes in the early phase of the test and by temperature gradient and gas mixture concentration difference after the pressure between the vessels has been equalized.

Therefore, the new tests, in addition to the intrinsic value of directly addressing a safety issue for a new reactor design, also provide with high quality data for code validation.

The calculations conducted with the GOTHIC code allow for assessment of the adequacy of using 3-D, coarse-mesh approach, which is required for full containment safety analysis, to predict the concentration evolution and the final gas distribution resulting from a high-velocity jet in a multi-compartment geometry. Moreover these simulations aim at complementing the interpretation of the physical phenomena taking place during the test evolution and inferred by the measurement results.

Some of the axis scales in the figures of the paper are not shown due to the confidential nature of the data. Nevertheless the present overview should allow the reader to follow and understand the main phenomena characterizing the evolution of the tests.

2. The PANDA facility

PANDA is a large-scale thermal-hydraulic test facility designed for investigating containment system behaviour, related phenomena for different ALWR designs, e.g. SBWR or ESBWR, and for large-scale separate effect tests. The containment compartments (i.e. Drywell (DW), Suppression Chamber or Wetwell (WW), Gravity Driven Cooling System (GDCS) and the Reactor Pressure Vessel (RPV)) simulated by six cylindrical pressure vessels, the Passive Cooling Condensers (PCCs) and the Isolation Condenser (IC) simulated by four condensers immersed in water pools are presented in Figure 1-(a). The overall height of the PANDA facility is 25 m, the total volume of the vessels is about 460 m³ and the maximum operating conditions are 10 bar at 200 °C. The RPV is equipped with an electrical heater bundle with a maximum power of 1.5 MW. Various auxiliary systems are available to maintain and control the necessary initial and boundary conditions during the tests. For the ST6 series only a part of the PANDA facility has been used, underlined in red in Figure 1-(a).

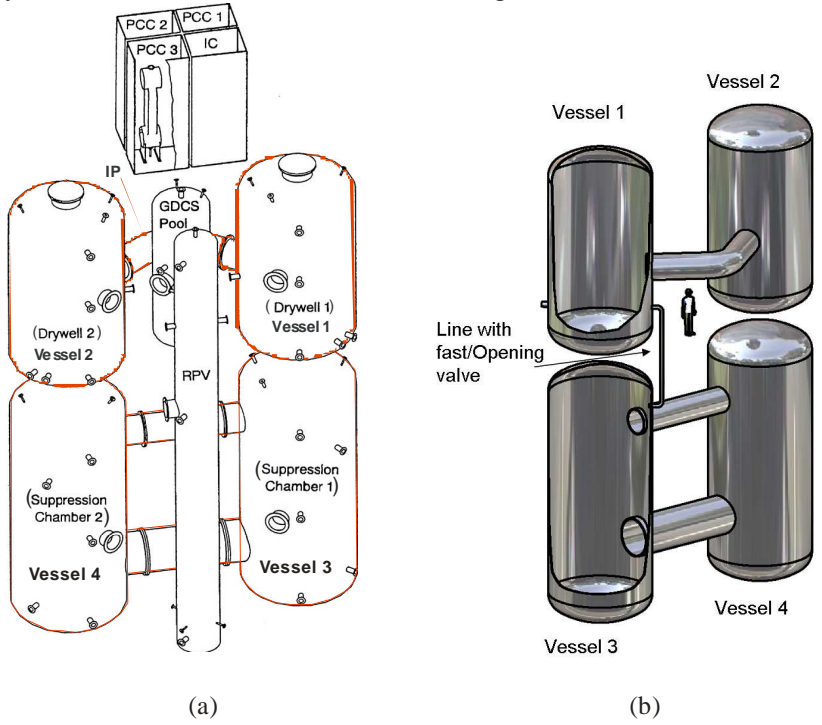


Figure 1: PANDA facility schematic (a) and facility configuration for ST6 series (b).

2.1 Configuration for ST6

A schematic for the PANDA configuration for ST6 series is shown in Figure 1.

Vessels 1 and 2¹ form the first volume (185 m³), whereas Vessels 3 and 4¹ form the second volume (254 m³). The line connecting both volumes, labeled VBL² hereafter, is about 15 m long and a difference in elevation of 5.4 m is assessed between its inlet and outlet.

2.2 Instrumentation for ST6

The PANDA instrumentation consists of more that 1000 sensors which allow for the measurement of fluid and wall temperatures, absolute and differential pressures, flow rates, heater power, gas concentrations. The measurement sensors are implemented in all the facility compartments, in the system lines and in the auxiliary systems.

With respect to the OECD/SETH-2 PANDA ST6 series the most relevant sensors are gas mixture concentration, wall and fluid temperature in Vessels 1 to 4. It should be pointed out that the accuracy for the temperature measurement is about $0.5~^{\circ}$ C. For the gas concentration measurements is estimated in case of a three gas mixture an error of about $\pm 1.5\%$.

3. ST6 test procedure and initial conditions

The ST6 series consisted of three PANDA tests named ST6_0, ST6_1 and ST6_2. The two volumes, Vessels 1-2 and Vessels 3-4, were first individually preconditioned with different gas compositions, temperatures and pressures. The test was then initiated with the opening of a fast opening valve located in the VBL between Vessel 1 and Vessel 3 (Figure 1-(b)). The main parameters for these tests are summarized in Table 1.

All three tests were conducted with the same facility configuration, and varying the initial conditions, Figure 2:

- <u>ST6_0</u>: Vessels 1-2-3-4 were filled with air. Vessels 1-2 were initially at room temperature and atmospheric pressure. Vessels 3 and Vessel 4 were at room temperature and pressurized (Vessels 3-4 pressure higher that Vessels 1-2 pressure).
 - <u>Specific objectives</u>: To observe the phenomena induced by the opening of the VBL valve, e.g. heating-up, density stratification, gas transport under quasi-adiabatic pressure transient conditions.
- <u>ST6_1</u>: Vessels 1-2 were filled with air at room temperature and atmospheric pressure. Vessels 3-4 were filled with a gas mixture of air-steam-helium and pressurized (i.e. Vessels 3-4 pressure and temperature higher that in Vessels 1-2).
 - <u>Specific objectives:</u> To observe the phenomena induced by the opening of the VBL valve, e.g. heating-up, density stratification, gas transport with possible condensation under pressure transient conditions.
- <u>ST6_2</u>: Vessels 1-2 were filled with air at atmospheric pressure. Vessels 3-4 were filled with a gas mixture of air-steam-helium and pressurized (i.e. Vessels 3-4 pressure higher that Vessels 1-2

¹ Vessels 1-2, in the PANDA terminology are those vessels representing the DW and Vessels 3-4 the WW of ESBWR. For the ST6 series the Vessels 1-2-3-4 do not have any relation with the DW and WW of the ESBWR

² VBL: is in the PANDA terminology the Vacuum Breaker Line of ESBWR. For the ST6 series the VBL does not have any relation with the DW and WW of the ESBWR

pressure). Similar temperatures were obtained for both fluid and structures in Vessels 1-2-3-4. Specific objectives: To observe the phenomena induced by the opening of the VBL valve, e.g. heating-up, density stratification, gas transport under pressure transient conditions with no condensation. Condensation was hindered by heating up Vessels 1 and 2 and the VBL.

Table 1: Main initial parameters for the ST6 series **ST6 1 ST6 2 ST6 0** Vessels 1-2: Air Air Air Composition: Temperature: Room Room Heated Pressure: Atmospheric Atmospheric Atmospheric Vessels 3-4: Composition: Air-steam-helium Air-steam-helium Air Temperature: Room Heated Heated Pressure: Pressurized Pressurized Pressurized Air Air Air Air Air room room room room Heated up Heated up temperature temperature temperature temperature atmospheric atmospheric atmospheric atmospheric atmospheric atmospheric pressure pressure pressure pressure CB.VBI CB.VB Vessel 1 CB.VB Vessel 2 Vessel 2 Vessel 1 Vessel 2 Vessel 1 VB line VB lin Air-Helium-Air-Helium-Air-Helium-Air-Helium-Steam Steam Steam Air Air Heated up Heated up room room Heated up Heated up temperature temperature Pressurized Pressurized Pressurized Pressurized Pressurized Pressurized Vessel 3 Vessel 3 Vessel 3 Vessel 4 Vessel 4 Vessel 4 ST6_0 ST6_1 ST6_2

Figure 2: Initial conditions in the ST6 series

4. Calculations using the GOTHIC code

The GOTHIC code is used for this paper to provide information that could help to gain some insight in the processes occurring during the tests. Due to space limitation, in this work only selected results will be presented, mainly related to Test ST6_2. The complete analysis will be reported in a future work. GOTHIC [11] is a general-purpose, thermal-hydraulics computer program, which solves separate conservation equations for mass, momentum and energy for three fields: a multi-component gas mixture, a continuous liquid, and droplets. In addition, species balances are solved for each component of the gas mixture. GOTHIC includes a full treatment of the momentum transport terms in multi-dimensional models, with optional models for turbulent shear, and for turbulent mass and energy

diffusion. In this work, the k-ε model has been used for representing turbulence. The hydraulic model of GOTHIC is based on a network of computational volumes (one, two or three-dimensional) connected by flow paths. In contrast to standard CFD packages, in GOTHIC the subdivision of a volume into a multi-dimensional grid is based on orthogonal co-ordinates. The 3-D capabilities of GOTHIC, to simulate basic flows of interest for containment analysis, have been extensively investigated (e.g., [12, 13]). The version of the code used in the present analysis is GOTHIC 7.2b.

Figure 3 shows the model used for simulating the tests of the ST6 series. It includes lumped parameter volumes for representing Vessels 3-4 (represented by a single volume due to the homogeneity of the conditions in these two vessels) and the VB line (divided in several segments to represent the various horizontal and vertical sections), and three subdivided volumes to represent Vessel 1, Vessel 2 and the IP, respectively. The nodalisation used for Vessel 1 is also shown in Fig. 3. Due to the cartesian mesh, the injection is perpendicular to the IP axis, instead of being at 80°. The nodalisation for Vessel 2 is similarly fine in the vertical direction, and much coarse in the two transversal directions.

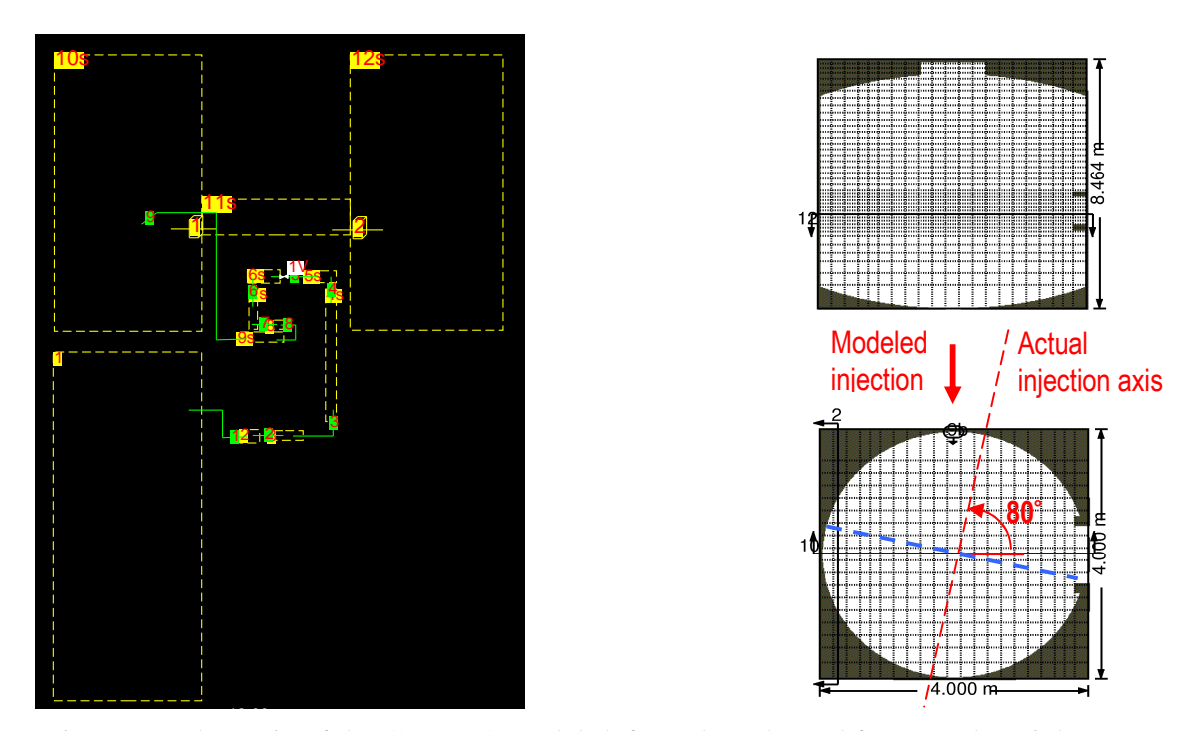


Figure 3: Schematic of the GOTHIC model (left) and mesh used for Vessel 1 (right).

5. ST6 test results

The test results presented in this section are discussed in term of pressure evolution, temperature and gas distribution. From these results, an attempt to infer the flow pattern developing during the evolution of the three PANDA tests (ST6_0, ST6_1, and ST6_2) is conducted. Comparisons of experimental data with GOTHIC simulations are also shown for the test ST6_2 for which a more detailed discussion of the experimental results is carried.

2-D temperature contour maps obtained by interpolating linearly with the closest neighbouring points the temperatures measured in Vessel 1 vertical cross section, in the IP and in Vessel 2 vertical cross section are shown in Figures 5 to 7. These temperature contour maps provide useful information on the flow patterns and evolutions in the containment during the conduction of the tests.

5.1 Boundary condition: VBL flow rate

Due to the test configuration, the main interest of the analysis resides in the gas transport and distribution observed in the two upper vessels (1 and 2). The GOTHIC prediction of the transient in Vessels 1 and 2, however, requires an accurate representation of the flow rate exiting from the VBL, which was not measured experimentally. An estimate of the flow rate was achieved by tuning the parameters describing the valve and the VBL in the GOTHIC model to reproduce accurately the depressurization of Vessels 3 and 4 for test ST6_1. The same parameters were used for all three tests. The measured pressure history as well as the one calculated by the code is presented in Figure 4 for tests ST6_1 and ST6_2. For reason of clarity test ST6_0 is not shown. However, a similarly good agreement was obtained. The very accurate representation of the pressure equalization process for all tests suggests that the flow rates were correctly predicted, so that the calculation of the transient in the two upper vessels was performed with fairly accurate boundary conditions. This permits to use the calculated results to complement the analysis of the experimental data with some considerations on the prevailing flow fields.

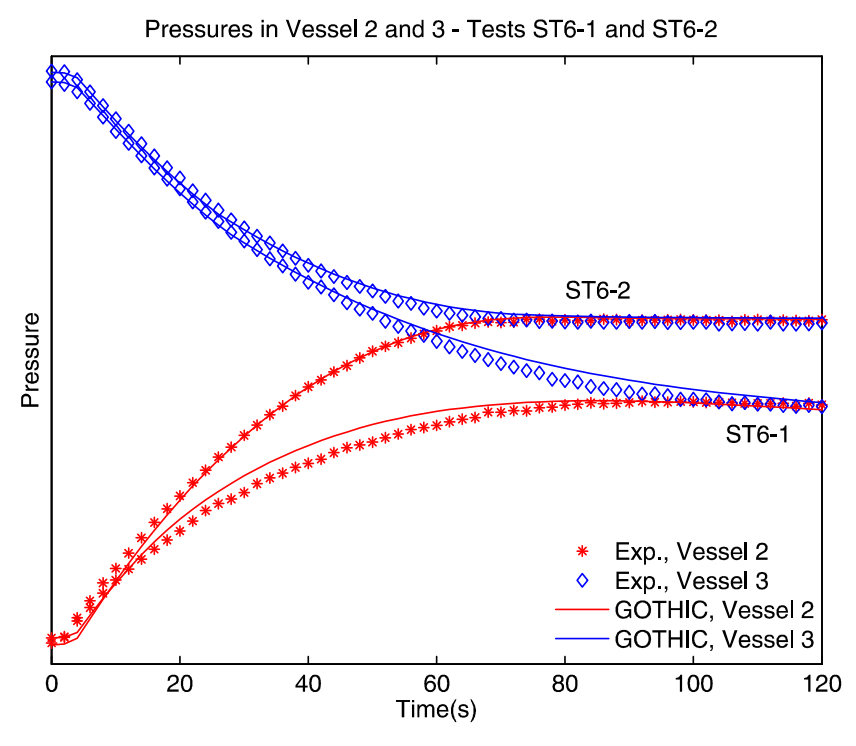


Figure 4: Pressures in Vessels 2 and 3 for Tests ST6_1 and ST6_2.

5.2 Test ST6_0

For the description of the test ST6_0 only the temperature measurements in the gas space of Vessels 1-2 and IP are used. Test ST6_0 has been performed with air only (Table 1). The pressure equalization (not shown in Figure 4) between the Vessels 1-2 and Vessels 3-4 was reached \sim 100 s after the opening of the valve in the VBL, similar to for test ST6_1.

Six 2D temperature contour maps obtained at 18s, 70s, 92s, 122s, 144s, 198s, respectively, are presented in Figure 5. In each frame the left-side vessel represents Vessel 1 whereas the right-side vessel represents Vessel 2. Within Vessel 1 a red dot indicates the elevation of the VBL exit. In this

representation, the outflow coming out from Vessel 3 enters Vessel 1 orthogonally to the measurement plane, see Figure 3.

One effect of Vessels 3-4 depressurization was the decrease of the gas temperature, while the pressurization of Vessels 1-2 is accompanied with a general increase in gas temperature.

The temperature contour maps, 18s and 70s, show that during the pressurization, the gas temperature increases in the upper region of Vessel 2 whereas no significant temperature change is observed in Vessel 1. This temperature difference between Vessels 1 and 2 is due to the different flow conditions in the two vessels: 1) in Vessel 1, a high momentum jet is created by the air flowing from Vessel 3. The temperature of the exiting jet is slightly colder than the one initially measured in Vessel 1 due to the decompression of the gas, which might tend to keep the overall temperature lower in the vessel. In addition, the high momentum jet induces mixing, therefore enhancing the heat transfer to the Vessel 1 wall. The latter is favoured to explain the small temperature change of Vessel 1. 2) In the mean time the air flowing to Vessel 2 through the IP has a much lower momentum. Very low heat transfer to the wall is expected there. Thus, due to the rapid pressure increase, Vessel 2 is experiencing a quasi-adiabatic process leading to a significant temperature increase. The temperature contour maps after pressure equalization (t > 100 s) show a general decrease in air temperature in both vessels.

The selected temperature contour maps at 92s, 122s, 144s, 198s reveal the presence of a colder region in the lower part of the IP (e.g. a flows from Vessel 1 to Vessel 2). In fact the air flowing from Vessel 1 to Vessel 2 is colder with respect to the air in the upper region of Vessel 2 and it accumulates in the lower region of Vessel 2. The warmer region in the upper part of the IP indicates the occurrence of a weak counter flow from Vessel 2 to Vessel 1 (>92s).

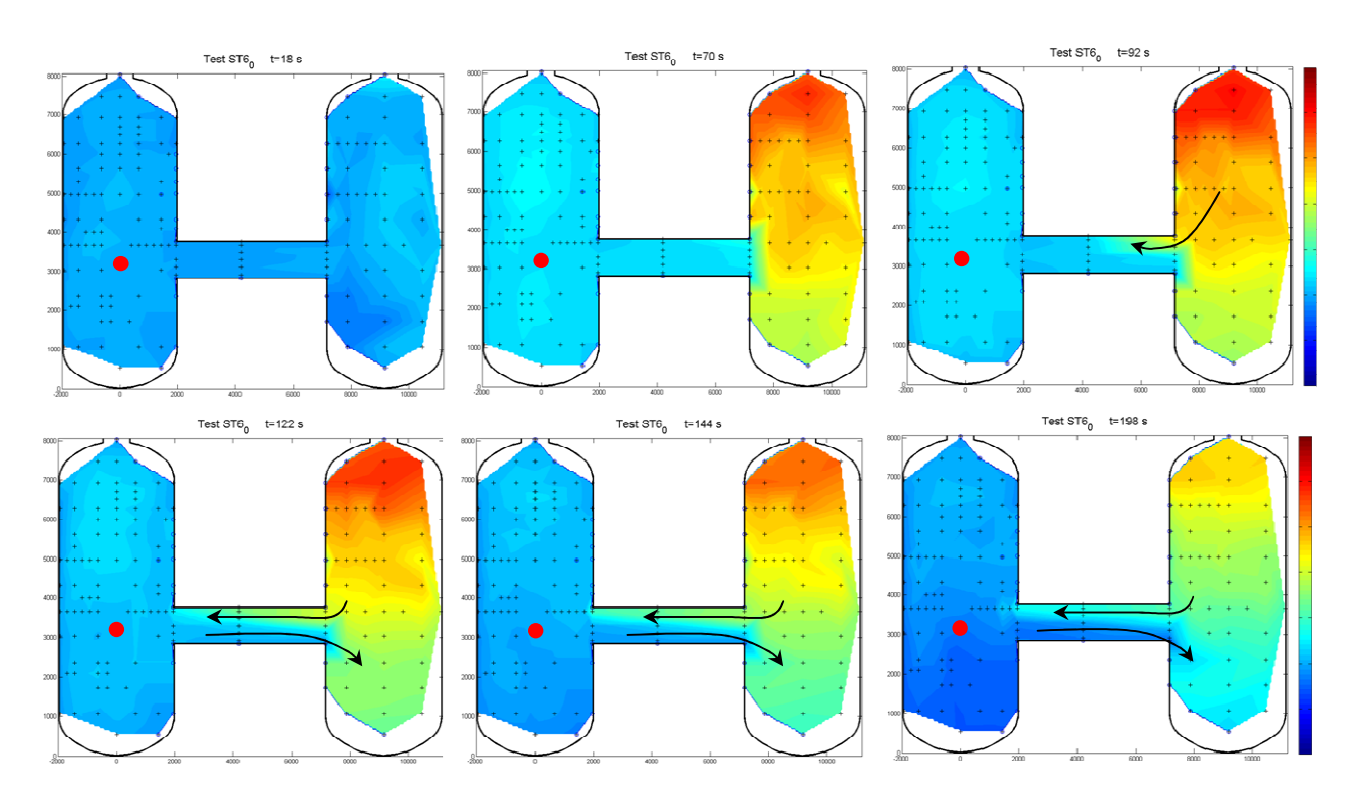


Figure 5: Temperature contour maps at selected times in test ST6_0

5.3 Test ST6_1

For the description of the test ST6_1 only the temperature measurements in the gas space of Vessels 1-2 and IP are used. Test ST6_1 has been performed with the Vessels 3 and 4 pressurized with a hot three gas mixture (Table 1). The VBL Vessel 1 and 2 were not heated up for test ST6_1. The pressure equalization between the Vessels 1-2 and Vessels 3-4 was reached ~ 100 s after the opening of the valve in the VBL, Figure 4. The pressure first equalizes in all four vessels and then slightly decreases as effect of steam condensation.

Six 2D temperature contour maps obtained at 14s, 40s, 64s, 130s, 182s, 280s, respectively, are presented in Figure 6. The overall representation of the temperature contour map is similar to the one described for test ST6_0.

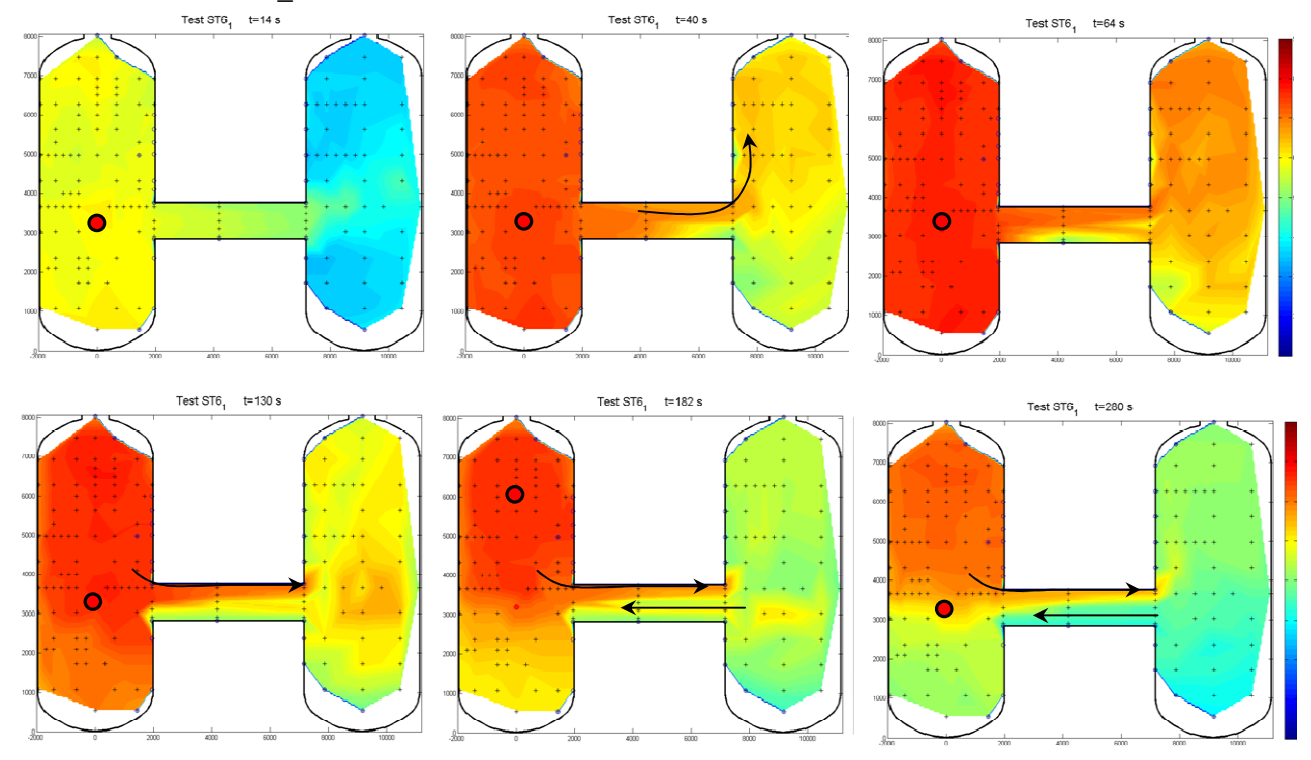


Figure 6: Temperature contour maps at selected times in test ST6_1

In the early phase of the test the flow through the VBL to Vessel 1 is jet-like and impinges on the Vessel 1 wall. The temperature contour map at 14 s shows a rather uniform gas temperature in Vessel 1. The temperature increase observed in Vessel 2 for ST6_0 due to pressurization is also expected in ST6_1. The initially large temperature difference between Vessel 1-2 and Vessel 3-4 hinders the observation of the temperature rise in Vessel 2 as the warm helium-rich gas mixture is transported from Vessel 1 through the IP to Vessel 2 (14s, 40s, and 64s). The filling of Vessel 2 with the lighter gas mixture starts from the upper region (40s) and progressively spreads to the lower region (64s, 130s). In the IP, a counter current flow is established(130s, 182s and 280 s) with "warmer and lighter mixture" flowing (in the upper region of IP) from Vessel 1 to Vessel 2, and a "colder and heavier mixture" flowing (in the lower region of the IP) from Vessel 2 to Vessel 1. The heavier mixture flowing to the lower region of Vessel 1 can be associated with a decrease in helium content.

At t=280s, the temperature map shows that the warmer mixture is confined at the top of Vessel 1 and in a thin portion of upper part of the IP while colder gas mixture is confined at the bottom of Vessel 2. The final temperature distribution shows stratification within each vessel resulting from complex intercompartment gas flow.

5.4 Test ST6 2

For the description of the test ST6_2, the temperature and gas concentration measurements in the gas space of Vessels 1-2 and IP are used. Test ST6_2 has been performed with the Vessels 3 and 4 pressurized with a hot three gas mixture (Table 1). The VBL and the Vessels 1-2 were heated up to the same temperature as Vessel 3-4 to avoid condensation during the test.

For this test, also simulations with the GOTHIC code will be discussed. In particular, the calculated final mixture compositions in the two Vessels 1-2 are compared with the experimental results and temperature, velocity and density fields at selected times will be shown. These simulations support the description of the phenomena provided below.

Six 2D temperature contour maps obtained at 30s, 42s, 76s, 126s, 300s, 600s, respectively, are presented in Figure 7. The overall representation of the temperature contour map is similar to the one described for test ST6_0 and ST6_1. The gas mixture compositions at selected locations of Vessel 1 and IP are presented in Figure 8.

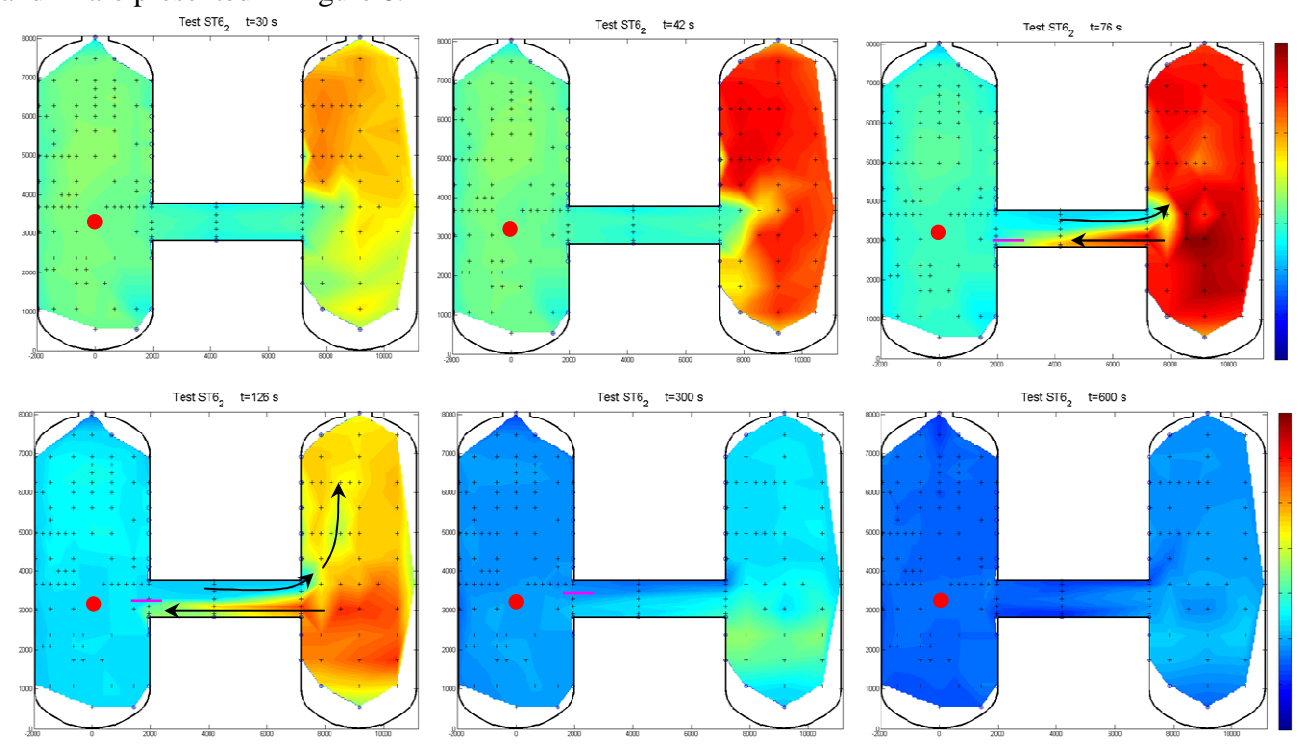


Figure 7: Temperature contour maps at selected times in test ST6_2

As all vessels are initially at the same temperature, one could expect behaviour similar to ST6_0 as long as the flow is not controlled by density change resulting from gas composition difference. In the early phase of the test (30s, 42s) the temperature contours map appears very similar to the one from ST6_0 characterized by a heating-up of Vessel 2 and a good mixing in Vessel 1, see section 5.2. This observation can also be inferred from the gas concentration measurements. In fact, in the early phase of the test the gas composition in the Vessel 1 (location A, F, T) and in the IP (location TD1-3) show a

uniform decrease in air concentration and increase in helium and steam concentrations (Figure 8) until t~ 60s, which results from a good mixing within the entire Vessel 1. Even though the pressure in the vessels does not equalized before t~75s (Figure 4), the gas composition measured at T level starts to deviate from the one from A and F level. This suggests that past 60s the decreasing momentum of the jet with time (following the decrease in pressure difference between Vessel 1-2 and Vessel 3-4) is not strong enough to ensure the mixing in the entire Vessel 1, Figure 10-(b). Gas stratification, and therefore density stratification, starts to appear in Vessel 1. Due to temperature and gas concentration distribution in the vessels, intercompartment gas transport continues beyond pressure equalization.

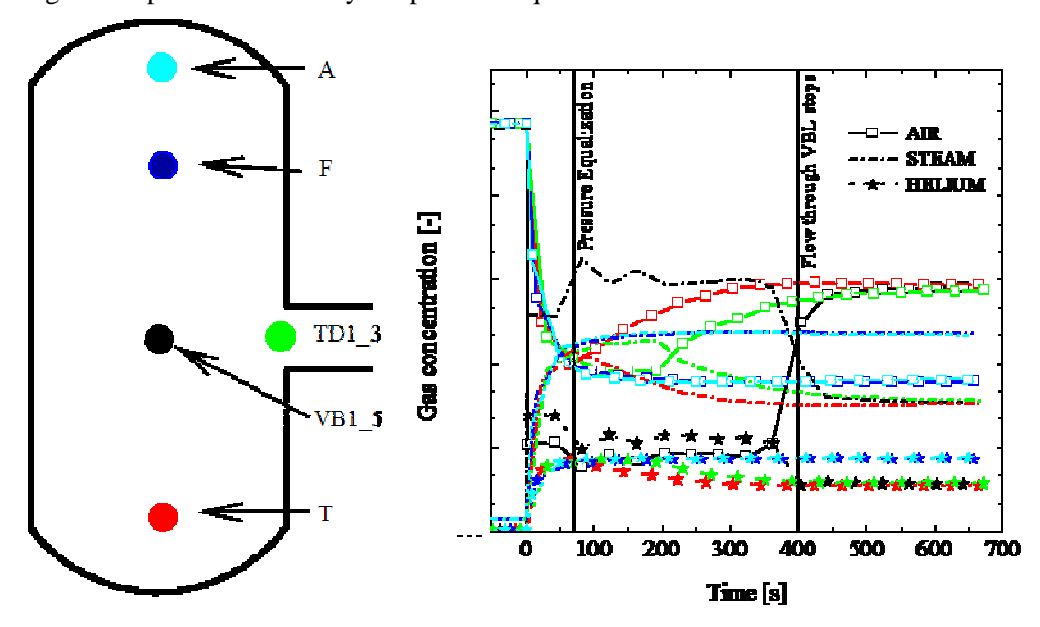


Figure 8: Trend for the gas mixture composition in Vessel 1 and IP in test ST6_2

At t=76s, a counter current flow appears in the IP with the three gas mixture flowing from Vessel 1 to Vessel 2 through the IP. As the Vessel 2 is mainly filled with air, the mixture flowing to Vessel 2 forms a buoyant plume which starts to fill the Vessel 2 upper region, Figure 7 t=126s. In the mean time warm air flows through the bottom of the IP from Vessel 2 to Vessel 1. The density of the gas mixture in the lower region of Vessel 1 increases.

At around 180s a change in the gas composition trend is observed in the IP at the sensor TD1-3. Until 180s TD1-3 gas composition measurement followed the one from A and F level. Past 180s the gas composition changes, the mixture become richer in air, while steam and helium decreases. The gas composition tends to reach the one of T level (at around 500s). It is suggested that at the sensor location TD1-3 the gas composition is influence by the gas mixture composition of the upper part of Vessel 1 prior to 180s. Past 180s the TD1-3 gas composition is influenced by the counter flow coming from Vessel through the IP. The interface between the two flows in the IP seems to move upward with time (see horizontal purple line delimiting the interface eon Figure 7). Similar discussion can be made for the VB1-5 sensor. Until t~400 s the gas composition corresponds to the one of Vessel 3-4 from which the flow come from. Past 400s the gas composition seems to reach value similar to the one of T level and TD1-3. It is suggested that the flow from Vessel 3-4 might have been interrupted. After t~450s the gas composition seems to become stable, which is also expressed with the homogeneous temperature measured at t=600s, Figure 7 and 8.

The main experimental trends illustrated above have been captured by the simulatiosn with the GOTHIC code, although some gas transport mechanisms could not be reproduced.

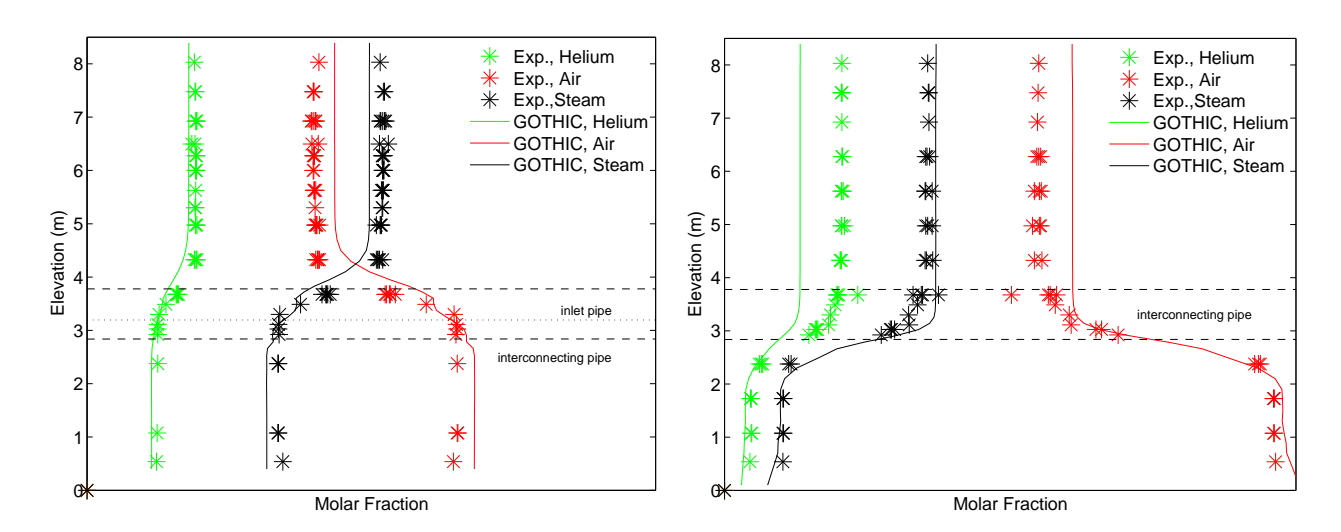


Figure 9: Final gas vertical distribution in Vessel 1 (left) and Vessel 2 (right).

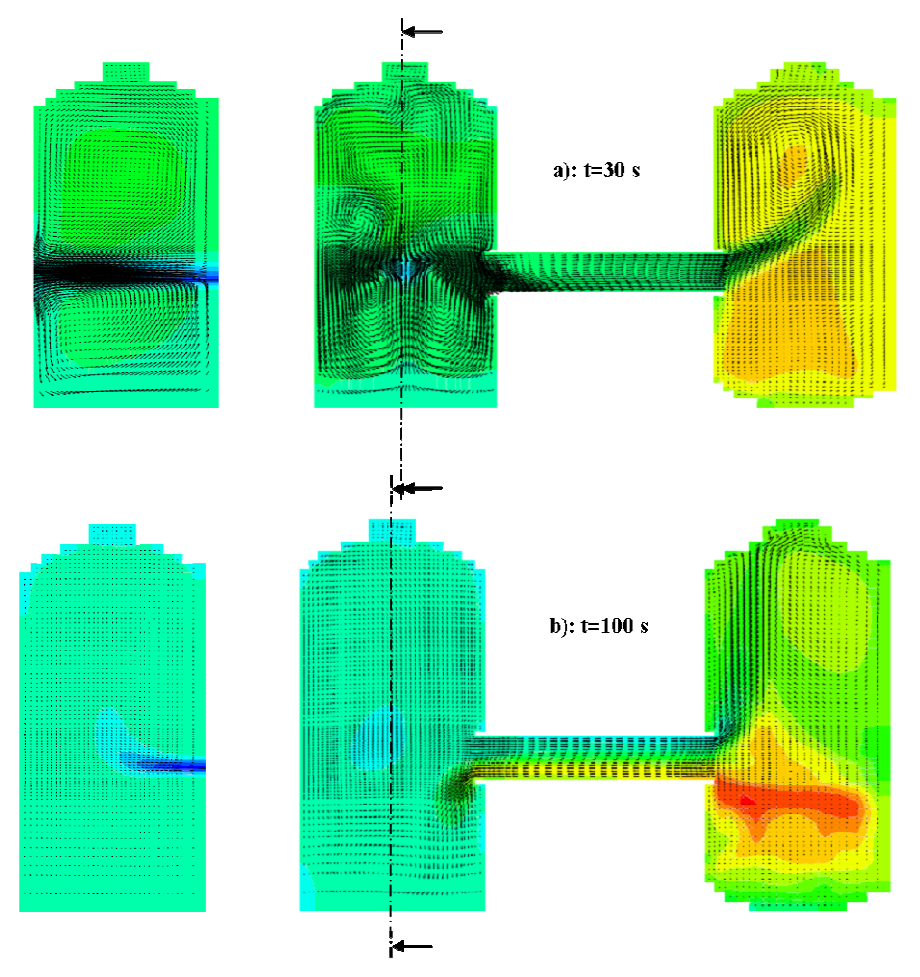


Figure 10: Temperature and velocity fields at two times during the early phase of test ST6_2.

In fact, the comparison of the predictions for the final gas distribution in Vessels 1 and 2 (Fig. 9) with the measured concentrations for test ST6_2 shows that the processes in Vessel 1 were accurately

represented. However, the final concentration of helium in the upper part of Vessel 2 was under predicted, which suggests that gas transport between Vessel 1 and 2 was not properly represented. These results suggest caution to use the code results for interpreting the test with respect to the flows in the IP and Vessel 2. This comparison, however, provides some confidence in the reliability of the predictions, and therefore some features of the flow prevailing in the tests can be obtained from the calculated results.

Figure 10 shows two snapshots of the flow field during the first 100 s obtained with GOTHIC, superimposed on the temperature contour. It has to be considered that at some locations the calculated temperatures strongly deviate from the measured values because of the difficulty of the code to predict heat transfer from the wall to the fluid when this is superheated [11]. This makes difficult to compare the results at time corresponding to those considered in Figure 7. Temperature is thus displayed for a qualitative description of its relation with the flow fields during the early phase of the transient.

In all tests, the flow from the VBL produces at the beginning of the transient a straight jet (Fig. 10a), which impinges on the opposite wall. The calculated velocities are initially higher than 100 m/s. The resulting effect of the high momentum jet discharging in Vessel 1 is to compress the fluid, which becomes increasingly warmer than the injected fluid. Due to the very efficient heat transfer with the structures caused by the high velocities, this increase is smaller than in Vessel 2, where the velocities are much smaller. The flow in the IP is in the same direction (from Vessel 1 to Vessel 2) at all elevations, with higher velocities at the bottom of the pipe (closer to the injection elevation), as momentum effects still dominate. Later in the transient (Fig. 10b) the velocities decrease: at time t=100 s they are already of the order of a few m/s, and the jet cannot impinge any longer the opposite wall due to the buoyancy effects, which bend the jet upward. At this time the temperature in Vessel 1 has become homogeneous. In the IP a counter-current flow is established, and a plume forms in Vessel 2. Under these conditions, the temperature in the lower zone of Vessel 2 is the highest in the fluid domain, similarly to the condition displayed in Fig. 7 at t=126 s.

The phase following the pressure equalization within the vessels is characterized by very low injection velocities (lower than 1 m/s) and rather uniform temperatures (see Fig. 7), and thus the flow is controlled by density differences. To illustrate this statement, the velocity field is shown in Fig. 11 together with the density field.

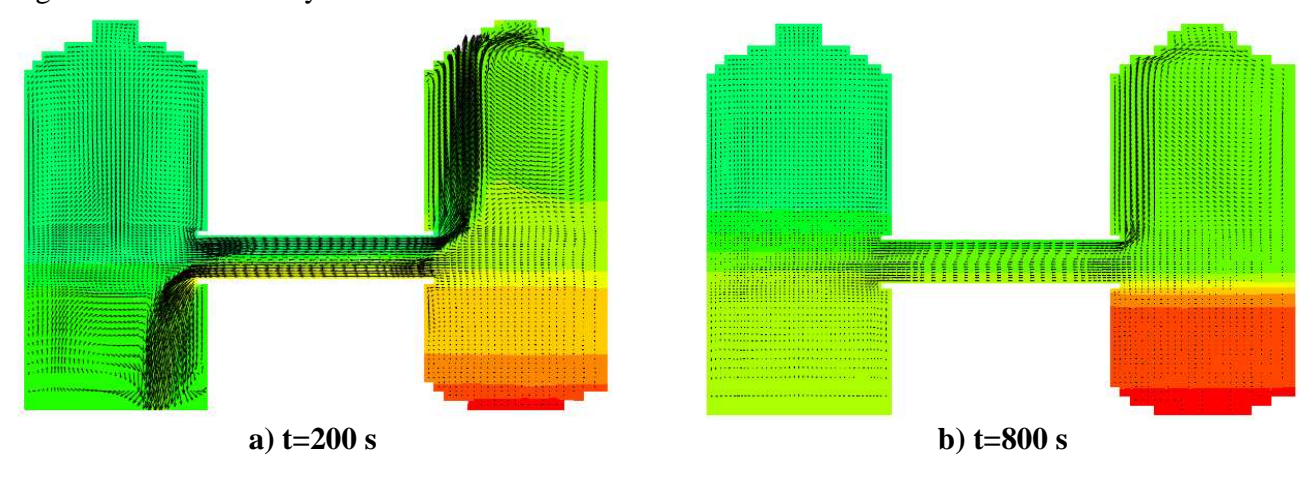


Figure 11: density and velocity fields at two times.

The scale for the vectors is different from that of Fig.10 for clarity of presentation. The snapshot at 200 s shows that light fluid from the upper part of Vessel 1 is transferred to Vessel 2 though the upper part of the IP. According to GOTHIC results, during this period the helium concentrations in the upper part

of both vessels tends to remain nearly equal. However, with the time passing the region of higher density (initially confined below the IP) rises above the top of the IP, and produces three-layer stratification.

The fluid transferred to the upper part of Vessel 2 has now the density (and the mixture composition) of the fluid in the middle layer, the communication between the upper parts of the two vessels being broken. Under these conditions, the calculated helium concentration in the upper part of Vessel 2 remains lower than that at the top of Vessel 1 until the end of the transient, in disagreement with the experimental trend (Fig. 9). It can be therefore inferred that in the test the boundary between the zones of lower and higher densities was below the top of the IP, which permitted the transfer of fluid from the top of Vessel 1 and thus an equalization of the helium concentrations.

6. Conclusion

The OECD/SETH-2 PANDA ST6 series presented in this paper, investigated at a large scale, the flow pattern and gas distribution in multi-compartment containment (Vessels 1-2 forms the first compartment, Vessels 3-4 forms the second compartment) after the sudden opening of a valve located in a line between the compartments. The gas transport and distribution within the compartments is driven in the early phase of the tests by the pressure difference within the compartments. When the pressure equalization is reached between Vessels 1-2 and Vessels 3-4, temperature and gas concentration gradients are present in the system. For the tests performed with three gases (ST6_1 and ST6_2), two main phases were distinguished: 1) from the start of the test until pressure equalization;2) from the pressure equalization up to the time when gas concentrations achieve nearly steady-state values in Vessels 1 and 2.

On the one hand, the analysis performed with the GOTHIC code, focused on test ST6_2 (and for the pressure transients ST6_1, ST6_2), and basically confirmed the aspects of the prevailing processes which could only be inferred from the temperature measurements and from the sparse information on mixture composition available. On the other hand, the good prediction of the pressure and the mixing in the receiving vessel showed that the code is able to predict the main phenomena associated with a fast flow produced by the sudden opening of a hatch. The inaccuracies of the simulation in predicting the final gas distribution in Vessel 2 revealed that inter-compartment gas transport is likely to be controlled by a continuous communication between the upper parts of both vessels, which could not be reproduced. This shows that the gas transport for conditions controlled by natural convection can be difficult to simulate using a coarse mesh and could require a more detailed nodalisation and/or more accurate models for turbulence and heat transfer with the structures.

The experimental data obtained with the ST6 series represent a unique database suitable to assess the capability of advanced LP and CFD codes to predict the gas transport between large volumes in a multi-compartment containment during transients controlled by large pressure gradients.

7. Acknowledgments

The authors gratefully acknowledge the support of all the countries and the international organizations participating in the OECD/SETH-2 project, the members of the Management Board and the Program Review Group of the SETH-2 projects.

The PANDA tests were performed with the technical contribution of Max Fehlmann, Chantal Wellauer and Wilhelm Bissels.

8. References

- [1] Agreement on the OECD/NEA SETH-2 Project, To resolve key computational issues for the simulations of thermal-hydraulic conditions in water reactor containments, OECD/NEA 2007.
- [2] R. Kapulla, D. Paladino, G. Mignot, R. Zboray and S. Gupta, "Break-up of Gas Stratified in LWR Containment Induced by Negatively Buoyant Jets and Plumes", In: Proceeding of the International Conference in Nuclear Engineering (ICONE17-75708), Brussels, Belgium, 2009 July 12-16.
- [3] G. Mignot, D. Paladino, R. Kapulla, R. Zboray, "Overview of vertical fluid release series" In: The 13th International Topical Meeting on Nuclear Reactor Thermal Hydraulics (NURETH-13), Kanazawa City, Ishikawa Prefecture, Japan, 2009 September 27-October 2.
- [4] R. Zboray, D. Paladino, G. Mignot, R. Kapulla, N. Erkan and M. Andreani, "Mixing of Density Stratified Containment Atmosphere by Horizontal Jet Release", In: International Conference Nuclear energy for New Europe 2009, Bled, Slovenia, 2009 September 14-17.
- [5] R. Zboray, G. Mignot, R. Kapulla, N. Erkan, D. Paladino, "Erosion and break-up of light-gas layers by horizontal injections in containment relevant atmosphere", International Conference on Nuclear Engineering ICONE19, May 16-19, 2011 Makuhari, Japan.
- [6] R. Kapulla, G. Mignot, D. Paladino, N. Erkan, R. Zboray, "Thermal-Hydraulic Phenomena Caused by the Interaction of Steam and Steam-Helium Mixture Wall Jets with a Containment Cooler", International Congress on Advances in Nuclear Power Plants (ICAPP 2011), Nice, France, 2011 May 2-5.
- [7] G. Mignot, R. Kapulla, N. Erkan, R. Zboray and D. Paladino, "Containment cooler performance in the presence of light non condensable gas with cooler location as a primary parameter", International Topical meeting on Nuclear Reactor Thermal-Hydraulics, (NURETH-14), Toronto, Ontario, Canada 2011 September 25-29 (submitted).
- [8] N. Erkan, G. Mignot, R. Zboray, D. Paladino, "Spray Tests in PANDA to Study Accident Mitigation in PWR Containment", In: International Conference Nuclear energy for New Europe 2009, Bled, Slovenia, 2009 September 14-17.
- [9] N. Erkan, G. Mignot, R. Kapulla, D. Paladino, R. Zboray, Effect of a containment spray application on the gas distribution with/without mass and heat transfer in two interconnected PANDA vessels", International Conference on Nuclear Engineering ICONE19, 2011 May 16-19, Makuhari, Japan (submitted).
- [10] R. P. Martin, C. A. Bonilla, E. S. Williams, "Combustible gas control system evaluation for the U.S. EPR", In: The 13th International Topical Meeting on Nuclear Reactor Thermal Hydraulics (NURETH-13), Kanazawa city, Ishikawa Prefecture, Japan, September 27-October 2, 2009, N13P1066
- [11] GOTHIC Containment Analysis Package, Version 7.2b(QA), EPRI, Palo Alto, CA, March 2009.
- [12] M. Andreani and D. Paladino, "Simulation of gas mixing and transport in a multi-compartment geometry using the GOTHIC containment code and relatively coarse meshes", Nuclear Eng. Design, 240, 1506-1527 (2010).

The $14^{\rm th}$ International Topical Meeting on Nuclear Reactor Thermalhydraulics, NURETH-14 Toronto, Ontario, Canada, September 25-30, 2011

[13] M. Andreani, T. George and D. Paladino "Simulation of basic gas mixing tests with condensation in the PANDA facility using the GOTHIC code", Nuclear Eng. Design, 210, 1528-1547 (2010).